

Qing-Feng Li, Min-Jie Li, Hai-Xia Lin*, Pei-Pei Xu, Ze-Bin Gu and Yong-Mei Cui*

Synthesis, optical and electrochemical properties of 2-[(9*H*-fluoren-2-yl)aryl]-1*H*-benzo[*d*]imidazole and 2,7-bis[(1*H*-benzo[*d*]imidazol-2-yl)aryl]-9*H*-fluorene derivatives

DOI 10.1515/hc-2015-0124

Received June 26, 2015; accepted August 12, 2015

Abstract: A series of 2-[(9*H*-fluoren-2-yl)aryl]-1*H*-benzo[*d*]imidazoles **11–13** and 2,7-bis[(1*H*-benzo[*d*]imidazol-2-yl)aryl]-9*H*-fluorenes **14–16** containing different linking aromatic units were synthesized in good yields. Their absorption and fluorescence properties were investigated in solution and in the solid state. Most compounds possess good fluorescence-emitting ability with ϕ_{FL} values in the region of 0.31–0.99 in solution and display strong blue emission. Structure–optical behavior characteristics and further details of the electronic properties from cyclic voltammetry measurements and theoretical calculations are discussed.

Keywords: 1*H*-benzo[*d*]imidazole; fluorene; structure-optical behavior.

Introduction

Fluorescent heterocyclic compounds are of interest as emitters for electroluminescence devices, molecular probes for biochemical research, dyes for textiles and polymers, fluorescent whitening agents and photoconducting materials [1–9] among other things. In particular, imidazole derivatives including phenylbenzo[*d*]imidazoles [10–21] and 1,3,5-tris(1-phenylbenzo[*d*]imidazol-2-yl)benzene (TPBI) have found applications in electrical and optical materials [22–24].

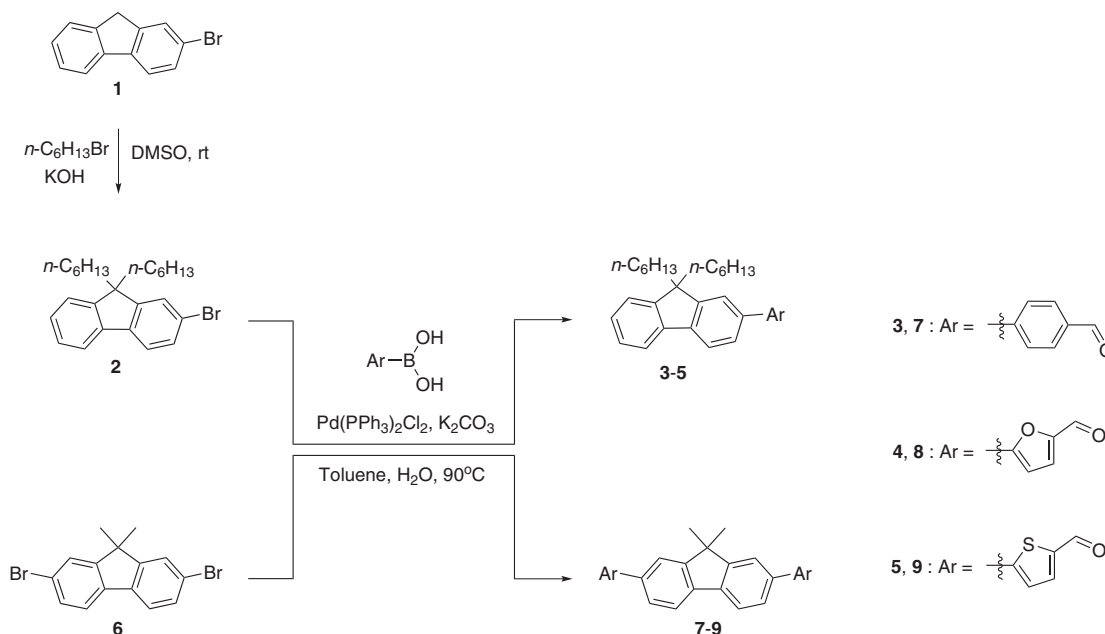
Due to their rigid oligophenyl unit within the molecular backbone and the possibility of facile functionalization at the methylene bridge, fluorene-based derivatives, including polymers and oligomers, are important as luminescent materials [19, 25–28], as well as carrier transport materials for field effect transistors (FETs) [29–31]. Their fluorescent characteristics rely largely on molecular structure and molecular assembly. Changes in the substitution pattern, conjugation, and molecular electronic structure can bring about very different optical and physical properties for such materials. There is presently a great interest to increase the structural or spatial dimensions of π conjugated molecules in order to acquire more favorable physical properties. In continuation of our efforts in synthesizing various fluorescent small molecules [32–35], in this paper we describe molecular combinations of fluorene and benzo[*d*]imidazole linked by π -conjugated moiety. We report the structure-optical behavior characteristics and further details of the electronic properties from cyclic voltammetry measurements and theoretical calculations of novel 2-[(9*H*-fluoren-2-yl)aryl]-1*H*-benzo[*d*]imidazole derivatives **11a–c**, **12a,b**, **13a,b** and 2,7-bis[(1*H*-benzo[*d*]imidazol-2-yl)aryl]-9*H*-fluorene derivatives **14a–c**, **15a,b**, **16a,b**. Extended conjugation is believed to result in intermolecular stacking interactions which are detrimental to the emission characteristics. Therefore, two *n*-hexyl or two methyl groups were introduced to the C-9 position of the fluorene moiety to increase solubility as well as to hinder intermolecular π - π stacking.

Results and discussion

The key aldehyde intermediates **3–5** and **7–9** were prepared as shown in Scheme 1. The bromo precursors **2** and **6** were conveniently converted to the arylated aldehyde derivatives **3–5** and **7–9** in 70–80% yields by treatment with the corresponding boronic acids in the presence of $\text{PdCl}_2(\text{PPh}_3)_2$ and K_2CO_3 under the Suzuki reaction

*Corresponding authors: Hai-Xia Lin and Yong-Mei Cui, Department of Chemistry, Innovative Drug Research Center, College of Sciences, Shanghai University, 99 Shangda Road, Baoshan District, Shanghai 200444, China, e-mail: haixialin@staff.shu.edu.cn (Hi-Xi Lin); ymcui@shu.edu.cn (Y.-M. Cui)

Qing-Feng Li, Min-Jie Li, Pei-Pei Xu and Ze-Bin Gu: Department of Chemistry, Innovative Drug Research Center, College of Sciences, Shanghai University, 99 Shangda Road, Baoshan District, Shanghai 200444, China



Scheme 1 Synthesis of the aldehyde intermediates.

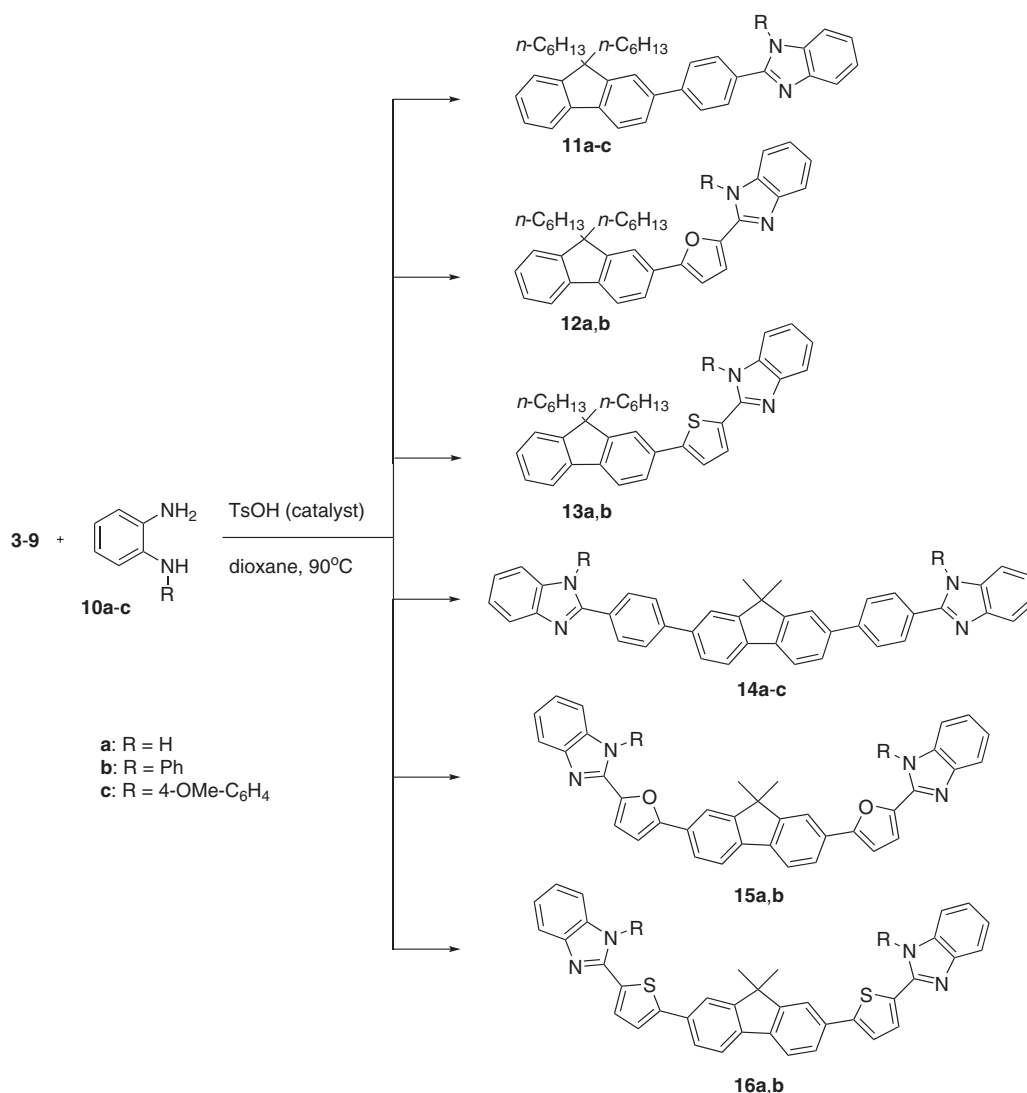
conditions [36]. Condensation of **3–5** or **7–9** with the diaminobenzene derivatives **10** in dioxane at 110°C for 2–5 h afforded the target compounds **11a–13b** and **14a–16b** in 60–80% yields (Scheme 2). All target compounds were purified by column chromatography on silica gel and their molecular structures were confirmed by ^1H NMR, ^{13}C NMR, and HR-MS.

The ORTEP view of the structure of **11b** in Figure 1A indicates that the moieties of fluorene, phenylene and 2-phenyl-1*H*-benzo[*d*]imidazole are non-coplanar with dihedral angles of 7.829° and 33.613°, respectively. In compound **13b**, as shown in Figure 2A, the fluorene moiety forms torsion angle of 13.100° with the adjacent thiophene ring ii, and the thiophene ring ii forms a torsion angle of 18.325° with the imidazole ring iii. The crystal packings of **11b** and **13b** are shown in Figures 1B and 2B. The molecules are stacked in the overlapping manner and face-to-face π - π intermolecular interactions between molecules can be regarded as the stacking force.

The photophysical properties of compounds **11a–13b** were examined using UV-vis absorption and fluorescence spectra in dilute solutions and in solid films. The absorption peak wavelengths (λ_{abs}) and the emission wavelengths (λ_{em}) are listed in Experimental. The emission spectra in the solid state were obtained for films spin-coated onto quartz from chloroform solution. All compounds show similar absorption profiles, principally owing to π - π^* transitions of the molecular backbone. Compounds **11a**, **12a**, **13a**, **14a**, **15a** and **16a** exhibit the absorption

maxima at 337 nm, 368 nm, 378 nm, 360 nm, 394 nm, and 400 nm in diluted CH_2Cl_2 solutions, respectively. The absorption maxima of **11a–16b** follow the order: **11a–c** (benzene) < **12a,b** (furan) < **13a,b** (thiophene) (Figure 3), **14a–c** (benzene) < **15a,b** (furan) < **16a,b** (thiophene). This result demonstrates that the heterocyclic ring plays an important role in the UV-vis absorption spectra due to the lone pair electrons which can cause n - π^* transitions with lower energy in the heteroatom (O, S). Compounds **14a–c**, **15a,b**, and **16a,b** have longer absorption wavelengths than **11a–c**, **12a,b**, and **13a,b** due to the elongation of conjugation. Compounds **15a,b** and **16a,b** exhibit the longest absorption wavelengths. Interestingly, compounds **11b,c**, **12b**, **13b**, **14b,c**, **15b** and **16b** with the phenyl or *para*-MeO substituted phenyl group in *N*-1 positions have almost the same absorption maxima as those of *N*-H compounds **11a**, **12a**, **13a**, **14a**, **15a** and **16a**, indicating that arylation of benz[*d*]imidazole has a limited effect on the energy levels of these compounds.

Theoretically, the absorption spectra caused by π - π^* transitions exhibit red shifts with the increase in solvent polarity. However, compounds **11a–16b** show blue-shifted absorption maxima by 5–26 nm in diluted MeOH solutions in comparison with the dilute CH_2Cl_2 solutions. The blue-shifted emission in MeOH may be ascribed to hydrogen-bonding interactions, which probably inhibits the reorientation of the benzo[*d*]imidazole in the excited state by hindering the rotation of the benzene, furan and thiophene subunits.

Scheme 2 Synthesis of **11a–16b**.

All compounds **11a–16b** display blue or blue-green emissions in dilute CH_2Cl_2 solutions (Figure 4). Compounds **11a**, **12a**, **13a**, **14a**, **15a** and **16a** show emission peaks at 452 nm, 456 nm, 461 nm, 457 nm, 463 nm and 496 nm, respectively. In contrast to the UV-vis absorption properties, the heteroatom (O, S) and the length of conjugation have less significant effects on the emission spectra of these compounds. A slight red-shift is observed for compounds **11c** and **14c** compared with their corresponding *N*-H analogues **11a** and **14a**. This result attests the partial involvement of the *N*-substituted chromophores in the electronically excited state. By comparison with the dilute CH_2Cl_2 solutions, the emission spectra of all compounds in MeOH solutions show shifts to shorter wavelengths by 37–68 nm, probably due to the hydrogen-bonding effects in MeOH solutions [37].

In comparison with the dilute CH_2Cl_2 solution, the emission spectra of compounds **11b,c**, **12b**, **13b**, **14b,c** and **15a,b** in solid state are shifted to shorter wavelengths by 10–53 nm. These compounds probably form *H*-aggregates, which decreases the π -conjugation significantly, in turn, resulting in the observed blue shift [38]. However, compounds **11a**, **12a** and **14a** show shift to longer wavelengths by 5–8 nm. The red shift of the emission observed in the solid state is probably due to the strong intermolecular forces, which drive the molecules to pack at high density to form *J*-aggregates with restricted molecular rotation and an increased π -conjugation, in turn, resulting in the red shift [39].

Most compounds show high fluorescence in CH_2Cl_2 solution with fluorescence quantum yields ϕ_{FL} in the range of 0.77–0.99 (Table 1). The relatively low quantum yields observed for compounds **13a,b** and **15a,b** with

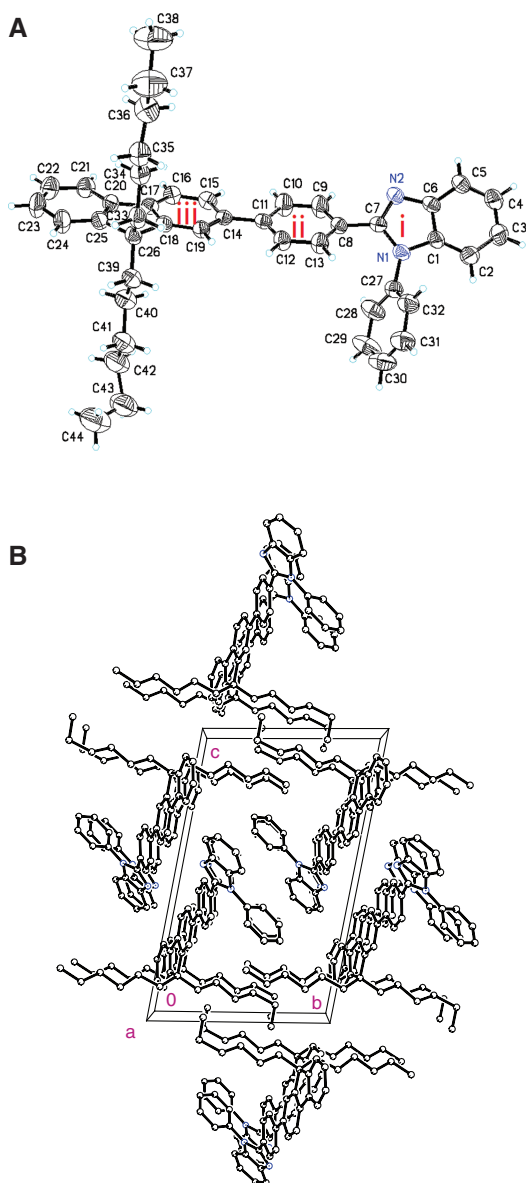


Figure 1 Molecular structures of compound **11b**.

The H atoms are omitted for clarity: (A) ORTEP drawing, (B) a view of the molecule packing structure.

heteroatoms suggest a fluorescence quenching caused by the heteroatom.

The redox potentials of all compounds were determined by cyclic voltammetry (CV) measurements which were carried out in a three-electrode cell setup with 0.1 M tetrabutylammonium perchlorate (Bu_4NClO_4) as a supporting electrolyte in anhydrous CH_2Cl_2 to probe the electrochemical behavior of the materials. The HOMO values were calculated as follows: $\text{HOMO} = [E_{\text{onset}}]_{\text{red/ox}} (\text{vs SCE}) + 4.6$, $E_g = 1240/\text{UV} (\text{onset})$ [40, 41]. As can be seen from Table 1, the band gaps (E_g) of about 2.51–2.92 eV were estimated from the optical edge. Compounds **12a–15b** exhibit relatively smaller band

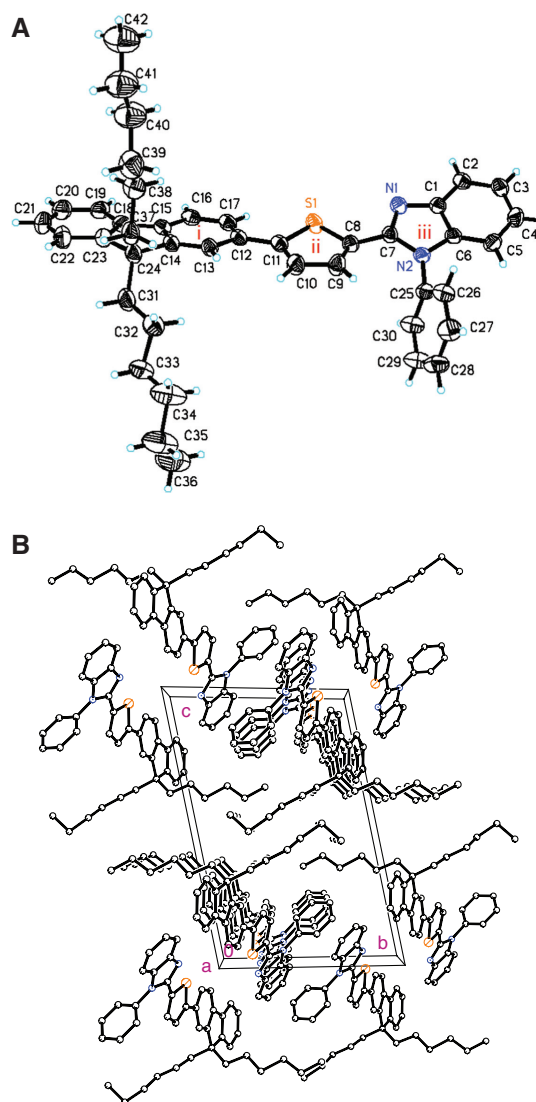


Figure 2 Molecular structures of compound **13b**.

The H atoms are omitted for clarity: (A) ORTEP drawing, (B) a view of the molecule packing structure.

gaps by comparison with compounds **11a–c**. The HOMO energies of these compounds were calculated by using the ferrocene/ferrocenium redox couple as a reference (4.6 eV) and were within the range of 5.43–5.84 eV. The LUMO energies were calculated from their corresponding HOMO energies and the optical band gap as estimated from the intersection of the absorption and emission peaks, which ranged from 2.59 eV to 3.36 eV. Compounds **14a–c** show relatively higher HOMO and LUMO energies than **11a–c**, probably due to the extended length of π -conjugation. However, in the case of **15a,b**, the HOMO and LUMO are lower in energy than those of **12a,b**; the ability of the heterocyclic ring (furan) to donate electrons is a possible explanation [42].

Density functional theory (DFT) calculations were also used to characterize the three-dimensional geometries

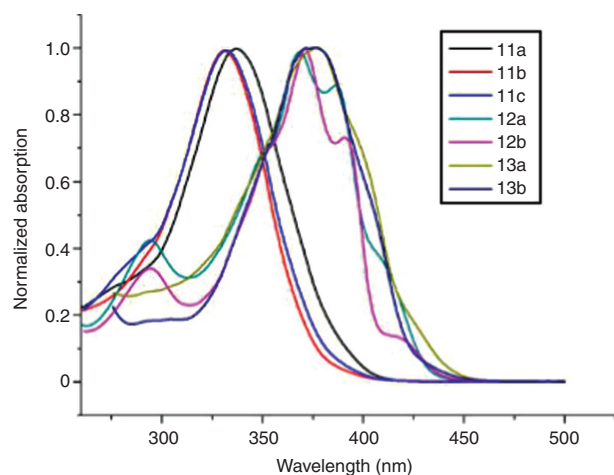


Figure 3 Normalized absorption spectra of **11a–13b** (1×10^{-5} M) recorded in CH_2Cl_2 .

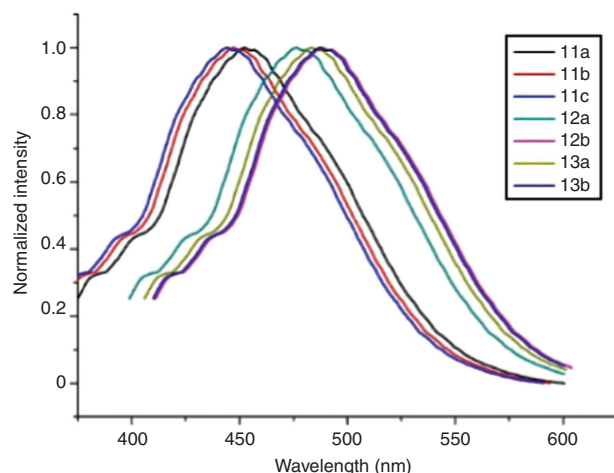


Figure 4 Normalized emission spectra of **11a–13b** (1×10^{-5} M) recorded in CH_2Cl_2 solutions; excitation at λ_{ex} at room temperature.

and the frontier molecular orbital energy levels of the representative compounds **11b**, **12b**, **13b** and **14b**, **15b**, **16b** at the B3LYP/6-31G* level by using the Gaussian 03 program [40, 41]. The orbital plots of the HOMO-LUMO are illustrated in Figure 5. In the case of compounds **11b**, **12b**, **14b**, **15b** and **16b**, the HOMO and LUMO are mainly localized on the fluorene and benzene (**11b**, **14b**), furan (**12b**, **15b**), and thiophene (**16b**) subunits, indicating that the absorption and emission processes are mostly attributed to the π - π^* transitions centered at the fluorene and aromatic moieties. Interestingly, compound **13b** spreads HOMO and LUMO through the thiophene subunit, which can explain the relatively high energy level. The LUMO of all compounds are not localized on the benzo[d]imidazole, which can explain the shorter-wavelength absorptions in polar solutions. The trends in the experimentally observed longer-wavelength absorptions for compounds **14b** and **15b** matches well the computed low-energy excitations.

Conclusions

2-[(9H-Fluoren-2-yl)aryl]-1H-benzo[d]imidazole and 2,7-bis[(1H-benzo[d]imidazol-2-yl)aryl]-9H-fluorene derivatives containing central aromatic or heteroaromatic subunits were conveniently synthesized in good yields. These compounds were thoroughly characterized by spectral and computational methods. Most compounds display emission in a blue region with ϕ_{FL} values in the range of 0.31–0.99. The HOMO energy levels of about 5.43–5.84 eV and the LUMO energy levels of about 2.59–3.36 eV were calculated. Further research regarding application of these systems as organic light-emitting diodes and as fluorescent probes is under way in our laboratory.

Table 1 Optical and electrochemical properties of compounds **11a–15b**.

Dye	ϕ_{FL}^a	HOMO ^b	LUMO ^c	E_g^d	Dye	ϕ_{FL}^a	HOMO ^b	LUMO ^c	E_g^d
11a	0.78	5.47	2.59	2.91	13b	0.60	5.82	3.14	2.68
11b	0.84	5.74	2.83	2.91	14a	0.54	5.84	3.36	2.48
11c	0.81	5.43	2.62	2.92	14b	0.99	5.75	2.94	2.81
12a	0.70	5.75	3.02	2.73	14c	0.99	5.72	2.90	2.82
12b	0.71	5.72	2.99	2.73	15a	0.31	5.59	3.00	2.51
13a	0.59	5.64	2.95	2.69	15b	0.38	5.43	2.81	2.62

^aFluorescence quantum yields measured in CH_2Cl_2 solution using a 0.1 M H_2SO_4 solution of quinine sulfate ($\phi_{\text{FL}} = 0.55$) as a reference.

^bHOMO energy levels derived from the oxidation potential using $E_{\text{HOMO}} = 4.6 + E_{\text{ox}}$, the redox potentials were measured with cyclic voltammetry system.

^cLUMO energy levels were deduced using the formula $E_{\text{LUMO}} = E_{\text{HOMO}} - E_g$.

^d $E_g = 1240/\text{UV}(\text{onset})$. UVs(onset) were estimated from the onset of the absorption spectra.

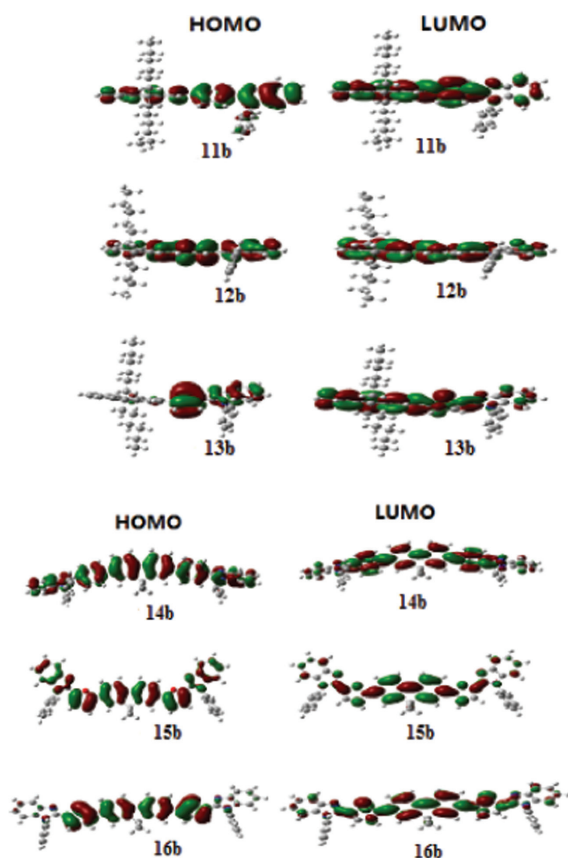


Figure 5 HOMO and LUMO electronic density distributions of **11b**, **12b**, **13b** and **14b**, **15b**, **16b**.

Experimental

Commercially available reagents were purchased and used without further purification. ^1H NMR (500 MHz) and ^{13}C NMR (125 MHz) spectra were recorded on a Bruker Avance spectrometer in CDCl_3 or $\text{DMSO}-d_6$. Chemical shifts in CDCl_3 were referenced to CHCl_3 (7.26 ppm) for ^1H NMR, and to CDCl_3 (77.16 ppm) for ^{13}C NMR. The center line of the multiplet of $\text{DMSO}-d_6$ was taken as δ 2.50 for ^1H NMR. Silica gel plates GF₂₅₄ were used for thin layer chromatography (TLC), and silica gel H or 300–400 mesh was used for flash column chromatography. Melting points were measured on a digital melting point apparatus without correction. The absorption and fluorescence spectra were recorded using a UV-2501Pc spectrophotometer and a RF-5301 fluorescence spectrophotometer, respectively. High-resolution mass spectra were recorded on a Bruker APEX III 7.0 instrument. The redox potentials of compounds were determined with cyclic voltammetry (CV) using a Base 2000 CV system. The HOMO values were recalculated from the reported literature values as $\text{HOMO} = [E_{\text{onset}}]_{\text{red/ox}} \text{ (vs SCE)} + 4.6$; $E_g = 1240/\text{UV (onset)}$.

General procedure for synthesis of 3–5

To a mixture of 2-bromo-9,9-dihexylfluorene (**2**) [34] (1 mmol), an aryl boronic acid (1.2 mmol), potassium carbonate (4 mmol) and

$\text{PdCl}_2(\text{PPh}_3)_2$ (0.1 mmol), was added toluene (9 mL) and water (1 mL) at room temperature. The mixture was heated to 90°C under nitrogen atmosphere for 8 h. After cooling, the mixture was extracted with ethyl acetate (10 mL). The organic extract was washed with saturated brine and dried over Na_2SO_4 . After removing the solvent, the crude product was purified by column chromatography on silica gel using ethyl acetate (1%–2%) in petroleum ether as eluent to afford the final product **3–5**.

4-(9,9-Dihexyl-9*H*-fluoren-2-yl)benzaldehyde (3) This compound was obtained from **2** and (4-formylphenyl)boronic acid; yellow oil; yield 80%; ^1H -NMR (CDCl_3): δ 10.11 (s, 1H), 8.02 (d, $J = 7.8$ Hz, 2H), 7.74 (m, 4H), 7.67 (s, 2H), 7.41 (m, 3H), 2.04–2.11 (m, 4H); ^{13}C -NMR (CDCl_3): δ 191.9, 151.7, 151.1, 147.7, 141.8, 140.4, 138.4, 135.1, 130.3, 129.0, 127.7, 127.5, 127.0, 126.4, 126.6, 120.2, 120.0, 55.3, 40.4, 31.5, 29.7, 23.8, 22.6, 14.0. HR-MS. Calcd for $\text{C}_{32}\text{H}_{38}\text{O}$ ($[\text{M} + \text{H}]^+$): m/z 439.3001. Found: m/z 439.2995.

5-(9,9-Dihexyl-9*H*-fluoren-2-yl)furan-2-carbaldehyde (4) This compound was obtained from **2** and (5-formylfuran-2-yl)boronic acid; yellow solid; yield 76%; ^1H -NMR (CDCl_3): δ 9.68 (s, 1H), 7.86 (d, $J = 1.3$ Hz, 1H), 7.77 (m, 3H), 7.37 (m, 4H), 6.91 (d, $J = 3.3$ Hz, 1H), 2.05 (m, 4H), 1.11 (m, 15H), 0.76 (t, $J = 7.3$ Hz, 6H), 0.59–0.68 (m, 4H); ^{13}C -NMR (CDCl_3): δ 177.0, 160.4, 151.9, 151.6, 143.0, 140.2, 127.9, 127.6, 127.0, 124.6, 123.0, 120.1, 119.5, 107.6, 55.4, 40.4, 31.5, 29.7, 23.7, 22.6, 14.0. HR-MS. Calcd for $\text{C}_{30}\text{H}_{36}\text{O}_2$ ($[\text{M} + \text{H}]^+$): m/z 429.2793. Found: m/z 429.2895.

5-(9,9-Dihexyl-9*H*-fluoren-2-yl)thiophene-2-carbaldehyde (5) This compound was obtained from **2** and (5-formylthiophen-2-yl)boronic acid; brown yellow solid; yield 71%; ^1H -NMR (CDCl_3): δ 9.92 (s, 1H), 7.79 (d, $J = 4.4$ Hz, 1H), 7.75 (m, 2H), 7.68–7.71 (m, 2H), 7.49 (d, $J = 4.3$ Hz, 1H), 7.37 (m, 3H), 2.02 (m, 4H), 1.01–1.17 (m, 15H), 0.77 (t, $J = 7.5$ Hz, 6H), 0.66 (m, 4H); ^{13}C -NMR (CDCl_3): δ 182.7, 155.3, 151.8, 151.1, 142.0, 140.1, 129.5, 127.8, 127.0, 126.4, 125.5, 124.1, 123.8, 123.0, 120.7, 120.3, 120.1, 55.3, 40.3, 31.4, 29.6, 23.7, 22.5, 14.0. HR-MS. Calcd for $\text{C}_{30}\text{H}_{36}\text{OS}$ ($[\text{M} + \text{H}]^+$): m/z 445.2565. Found: m/z 445.2535.

General procedure for synthesis of 7–9

To a mixture of 2,7-dibromo-9,9-dimethyl-9*H*-fluorene (**6**, 1 mmol), an aryl boronic acid (2.4 mmol), potassium carbonate (4 mmol), $\text{PdCl}_2(\text{PPh}_3)_2$ (0.2 mmol) was added toluene (9 mL) and water (1 mL) at room temperature. The mixture was heated to 90°C under nitrogen atmosphere for 24 h, then cooled and extracted with ethyl acetate (10 mL) and water (10 mL). The organic layer was washed with saturated brine and dried over Na_2SO_4 . After removing the solvent, the crude product was purified by column chromatography on silica gel using ethyl acetate (2%–3%)/petroleum ether as eluent to afford the final purified product **7–9**.

4,4'-(9,9-Dimethyl-9*H*-fluorene-2,7-diyl)bisbenzaldehyde (7) This compound was obtained from **6** and (4-formylphenyl)boronic acid; yellow solid; yield 70%; ^1H -NMR (CDCl_3): δ 10.10 (s, 2H), 8.01 (d, $J = 8.8$ Hz, 3H), 7.87 (m, 5 H), 7.71 (m, 5H), 7.46–7.52 (m, 1H), 1.64 (s, 6H); ^{13}C -NMR (CDCl_3): δ 191.9, 154.8, 147.4, 139.9, 135.1, 132.1, 128.6, 127.7, 121.6, 120.8, 47.2, 27.2. HR-MS. Calcd for $\text{C}_{29}\text{H}_{22}\text{O}_2$ ($[\text{M} + \text{Na}]^+$): m/z 425.1518. Found: m/z 425.1516.

5,5'-(9,9-Dimethyl-9H-fluorene-2,7-diyl)bis(furan-2-carbaldehyde) (8) This compound was obtained from **6** and (5-formylfuran-2-yl)boronic acid; yellow solid; yield 62%; $^1\text{H-NMR}$ ($\text{DMSO}-d_6$): δ 9.68 (s, 2H), 7.95 (s, 2H), 7.80–7.86 (m, 5H), 7.67–7.75 (m, 2H), 7.66–7.11 (m, 1H), 7.48 (m, 2H), 7.38 (d, $J = 4.4$ Hz, 2H), 6.94 (d, $J = 4.4$ Hz, 2H), 1.61 (s, 6H); $^{13}\text{C-NMR}$ ($\text{DMSO}-d_6$): δ 177.1, 159.8, 154.9, 152.0, 139.9, 132.1, 132.0, 131.9, 131.9, 128.5, 128.4, 128.4, 124.9, 120.9, 119.5, 107.8, 47.3, 26.9. HR-MS. Calcd for $\text{C}_{25}\text{H}_{18}\text{O}_4$ ($[\text{M} + \text{Na}]^+$): m/z 405.1103. Found: m/z 405.0640.

5,5'-(9,9-Dimethyl-9H-fluorene-2,7-diyl)bis(thiophene-2-carbaldehyde) (9) This compound was obtained from **6** and (5-formylthiophen-2-yl)boronic acid; yellow solid; yield 60%; $^1\text{H-NMR}$ ($\text{DMSO}-d_6$): δ 9.98 (s, 2H), 7.86 (s, 2H), 7.67 (m, 4H), 7.59 (m, 3H), 7.50 (m, 1H), 7.41 (m, 2H), 7.30 (d, $J = 4.2$ Hz, 2H), 6.95 (d, $J = 4.4$ Hz, 2H), 1.59 (s, 6H); $^{13}\text{C-NMR}$ ($\text{DMSO}-d_6$): δ 179.1, 163.6, 158.5, 156.0, 149.9, 145.1, 136.0, 135.6, 131.7, 126.5, 123.4, 123.4, 121.2, 119.9, 117.5, 107.1, 45.5, 23.3. HR-MS. Calcd for $\text{C}_{25}\text{H}_{18}\text{O}_2\text{S}_2$ ($[\text{M} + \text{Na}]^+$): m/z 437.0646. Found: m/z 437.0640.

General procedure for synthesis of 11a–c

To a mixture of 4-(9,9-dihexyl-9H-fluorene-2-yl)benzaldehyde (**3**, 0.7 mmol), benzene-1,2-diamine, *N*-phenylbenzene-1,2-diamine or *N*-(4-methoxyphenyl)benzene-1,2-diamine (**10a–c**, 1.0 mmol), and TsOH (0.1 mmol), was added dioxane (7 mL) at room temperature. The mixture was heated under reflux for 9 h, then concentrated, and the residue was purified by column chromatography on silica gel using ethyl acetate (5%–10%)/petroleum ether as eluent to afford the final product.

2-[4-(9,9-Dihexyl-9H-fluorene-2-yl)phenyl]-1H-benz[d]imidazole (11a) This compound was obtained from **3** and **10a**; yellow solid; yield 80%; mp > 400 °C; $^1\text{H-NMR}$ (CDCl_3): δ 8.20 (d, $J = 8.3$ Hz, 2H), 7.59–7.83 (m, 8H), 7.29–7.40 (m, 5H), 2.03 (m, 4H), 1.01–1.16 (m, 12H), 0.77 (t, $J = 7.4$ Hz, 6H), 0.68 (m, 4H); $^{13}\text{C-NMR}$ (CDCl_3): δ 151.5, 151.5, 151.0, 143.5, 138.7, 128.1, 127.7, 127.2, 126.8, 125.9, 122.9, 121.2, 120.0, 119.8, 55.2, 40.4, 47.2, 23.7, 22.5, 13.9; λ_{abs} (CH_2Cl_2) 337 nm, λ_{abs} (MeOH) 332 nm; λ_{em} (CH_2Cl_2) 452 nm, λ_{em} (MeOH) 400, 397 nm, λ_{em} (film) 460 nm. HR-MS. Calcd for $\text{C}_{38}\text{H}_{45}\text{N}_2$ ($[\text{M} + \text{H}]^+$): m/z 527.3426. Found: m/z 527.3426.

2-[4-(9,9-Dihexyl-9H-fluorene-2-yl)phenyl]-1-phenyl-1H-benz[d]imidazole (11b) This compound was obtained from **3** and **10b**; white solid; yield 75%; mp 147–150 °C; $^1\text{H-NMR}$ (CDCl_3): δ 7.96 (d, $J = 7.7$ Hz, 2H), 7.51–7.78 (m, 11H), 7.27–7.43 (m, 8H), 2.02 (t, $J = 8.6$ Hz, 4H), 1.09 (m, 12H), 0.77 (t, $J = 7.3$ Hz, 6H), 0.68 (m, 4H); $^{13}\text{C-NMR}$ (CDCl_3): δ 152.1, 151.5, 150.9, 143.0, 142.5, 140.9, 140.6, 138.8, 137.4, 137.1, 129.9, 128.6, 128.5, 127.5, 127.2, 126.9, 126.8, 125.9, 123.3, 122.9, 119.9, 119.8, 110.4, 55.2, 40.4, 31.4, 29.7, 23.7, 22.5; λ_{abs} (CH_2Cl_2) 332 nm, λ_{abs} (MeOH) 328 nm; λ_{em} (CH_2Cl_2) 468 nm, λ_{em} (MeOH) 405 nm and 425 nm, λ_{em} (film) 444.9 nm. HR-MS. Calcd for $\text{C}_{44}\text{H}_{46}\text{N}_2$ ($[\text{M} + \text{H}]^+$): m/z 603.3739. Found: m/z 603.3738.

2-[4-(9,9-Dihexyl-9H-fluorene-2-yl)phenyl]-1-(4-methoxyphenyl)-1H-benz[d]imidazole (11c) This compound was obtained from **3** and **10c**; white solid; yield 70%; mp 128–130 °C; $^1\text{H-NMR}$ (CDCl_3): δ 7.93 (d, $J = 8.5$ Hz, 2H), 7.75 (m, 4H), 7.65 (d, $J = 9.3$ Hz, 2H), 7.59 (t, $J = 8.5$ Hz, 2H), 7.22–7.39 (m, 9H), 7.07 (d, $J = 8.0$ Hz, 2H), 3.92 (s, 3H),

2.01 (t, $J = 8.5$ Hz, 2H), 1.03 (m, 12H), 0.77 (t, $J = 7.4$ Hz, 6H), 0.62–0.70 (m, 4H); $^{13}\text{C-NMR}$ (CDCl_3): δ 159.6, 152.2, 151.4, 150.9, 142.4, 140.9, 140.6, 138.8, 137.7, 129.7, 128.7, 126.8, 126.8, 125.9, 123.2, 122.9, 122.9, 121.2, 119.9, 119.8, 119.6, 115.1, 110.4, 55.5, 55.1, 40.4, 31.4, 29.6, 23.7, 22.5, 13.9; λ_{abs} (CH_2Cl_2) 333 nm, λ_{abs} (MeOH) 326 nm; λ_{em} (CH_2Cl_2) 462 nm, λ_{em} (MeOH) 401 nm and 425 nm, λ_{em} (film) 452 nm. HR-MS. Calcd for $\text{C}_{45}\text{H}_{48}\text{N}_2\text{O}$ ($[\text{M} + \text{H}]^+$): m/z 633.3845. Found: m/z 633.3833.

General procedure for synthesis of 12a,b and 13a,b

To a mixture of 5-(9,9-dihexyl-9H-fluorene-2-yl)furan-2-carbaldehyde (**4**, 0.7 mmol) or 5-(9,9-dihexyl-9H-fluorene-2-yl)thiophene-2-carbaldehyde (**5**, 0.7 mmol), benzene-1,2-diamine (**10a**, 1.0 mmol) or *N*-phenylbenzene-1,2-diamine (**10b**, 1.0 mmol), and TsOH (0.1 mmol) was added dioxane (7 mL) at room temperature. The mixture was heated under reflux for 9 h. The solvent was removed under reduced pressure and the crude product was purified by column chromatography on silica gel using ethyl acetate (10%–14%)/petroleum ether as eluent to afford the final product **12** or **13**.

2-[5-(9,9-Dihexyl-9H-fluorene-2-yl)furan-2-yl]-1H-benz[d]imidazole (12a) This compound was obtained from **4** and **10a**; yellow solid; yield 65%; mp 203–206 °C; $^1\text{H-NMR}$ (CDCl_3): δ 7.74 (m, 5H), 7.34 (m, 6H), 6.90 (d, $J = 3.6$ Hz, 2H), 2.01 (m, 4H), 1.08 (m, 12H), 0.76 (t, $J = 8.5$ Hz, 6H), 0.62 (m, 4H); $^{13}\text{C-NMR}$ (CDCl_3): δ 156.1, 151.4, 150.9, 143.8, 141.5, 140.4, 128.4, 127.4, 126.8, 123.3, 123.2, 122.8, 120.0, 119.8, 118.3, 113.3, 107.6, 55.2, 40.4, 31.5, 29.7, 23.7, 22.5, 13.9; λ_{abs} (CH_2Cl_2) 368 nm, λ_{abs} (MeOH) 364 nm; λ_{em} (CH_2Cl_2) 456 nm, λ_{em} (MeOH) 394 nm and 417 nm, λ_{em} (film) 464 nm. HR-MS. Calcd for $\text{C}_{36}\text{H}_{40}\text{N}_2\text{O}$ ($[\text{M} + \text{H}]^+$): m/z 517.3219. Found: m/z 517.3217.

2-[5-(9,9-Dihexyl-9H-fluorene-2-yl)furan-2-yl]-1-phenyl-1H-benz[d]imidazole (12b) This compound was obtained from **4** and **10b**; yellow solid; yield 60%; mp 92–96 °C; $^1\text{H-NMR}$ (CDCl_3): δ 7.94 (d, $J = 9.5$ Hz, 2H), 7.69 (m, 4H), 7.64 (d, $J = 9.4$ Hz, 1H), 7.56 (d, $J = 7.6$ Hz, 2H), 7.37 (m, 5H), 7.26 (m, 2H), 7.15 (d, $J = 8.8$ Hz, 1H), 6.77 (d, $J = 3.4$ Hz, 1H), 1.95–2.10 (m, 4H), 1.02–1.20 (m, 12H), 0.80 (t, $J = 7.4$ Hz, 6H), 0.57–0.65 (m, 4H); $^{13}\text{C-NMR}$ (CDCl_3): δ 156.2, 151.2, 150.8, 144.1, 143.1, 141.2, 140.5, 137.3, 137.1, 129.8, 129.3, 128.5, 128.1, 127.3, 126.8, 123.4, 123.2, 123.2, 122.8, 119.8, 119.7, 119.5, 118.0, 115.2, 110.2, 106.2, 106.8, 55.2, 40.4, 31.5, 29.7, 23.6, 22.6, 14.0; λ_{abs} (CH_2Cl_2) 371 nm, λ_{abs} (MeOH) 368 nm; λ_{em} (CH_2Cl_2) 469 nm, λ_{em} (MeOH) 426 nm, λ_{em} (film) 462 nm. HR-MS. Calcd for $\text{C}_{42}\text{H}_{44}\text{N}_2\text{O}$ ($[\text{M} + \text{H}]^+$): m/z 593.3532. Found: m/z 593.3538.

2-[5-(9,9-Dihexyl-9H-fluorene-2-yl)thiophen-2-yl]-1H-benz[d]imidazole (13a) This compound was obtained from **5** and **10a**; yellow solid; yield 65%; mp 189–192 °C; $^1\text{H-NMR}$ (CDCl_3): δ 7.72 (m, 3H), 7.65 (m, 2H), 7.60 (m, 2H), 7.33 (m, 4H), 7.28 (m, 2H), 1.99 (t, $J = 8.6$ Hz, 4H), 1.08 (m, 12H), 0.76 (t, $J = 7.4$ Hz, 6H), 0.66 (m, 4H); $^{13}\text{C-NMR}$ (CDCl_3): δ 151.6, 150.9, 148.2, 147.1, 141.5, 140.3, 132.1, 130.9, 127.9, 127.3, 126.8, 124.8, 123.6, 123.2, 123.2, 122.9, 120.1, 119.8, 55.1, 40.3, 31.4, 29.7, 29.6, 23.7, 22.5, 13.9; λ_{abs} (CH_2Cl_2) 378 nm, λ_{abs} (MeOH) 362 nm; λ_{em} (CH_2Cl_2) 461 nm, λ_{em} (MeOH) 425 nm, λ_{em} (film) 450 nm. HR-MS. Calcd for $\text{C}_{36}\text{H}_{40}\text{N}_2\text{S}$ ($[\text{M} + \text{H}]^+$): m/z 533.2990. Found: m/z 533.2988.

2-[5-(9,9-Dihexyl-9H-fluorene-2-yl)thiophen-2-yl]-1-phenyl-1H-benz[d]imidazole (13b) This compound was obtained from **5** and **10b**; green solid; yield 80%; mp 95–97 °C; $^1\text{H-NMR}$ (CDCl_3): δ 7.93

(d, $J = 8.8$ Hz, 1H), 7.64 (m, 9H), 7.35 (m, 4H), 7.26 (d, $J = 8.3$ Hz, 1H), 7.18 (d, $J = 4.8$ Hz, 1H), 7.11 (d, $J = 8.4$ Hz, 1H), 6.76 (s, 1H), 2.01 (t, $J = 16.6$ Hz, 4H), 1.10 (m, 12H), 0.79 (t, $J = 7.5$ Hz, 6H), 0.64–0.73 (m, 4H); $^{13}\text{C-NMR}$ (CDCl_3): δ 151.6, 151.0, 148.0, 147.0, 147.2, 141.4, 140.4, 137.7, 136.4, 132.2, 130.2, 129.7, 129.0, 128.3, 127.3, 126.8, 124.6, 123.4, 123.2, 123.2, 122.9, 120.3, 120.1, 119.8, 119.4, 110.1, 55.1, 40.4, 31.4, 29.7, 29.7, 23.7, 22.6, 14.0; λ_{abs} (CH_2Cl_2) 376 nm, λ_{abs} (MeOH) 364 nm; λ_{em} (CH_2Cl_2) 457 nm, λ_{em} (MeOH) 421 nm and 442 nm, λ_{em} (film) 450 nm. HR-MS. Calcd for $\text{C}_{42}\text{H}_{42}\text{N}_2\text{S}$ ($[\text{M}+\text{H}]^+$): m/z 609.3303. Found: m/z 609.3295.

General procedure for synthesis of 14a–16b

To a mixture of an aldehyde **7-9** (0.7 mmol), a benzene-1,2-diamine **10a-c** (1.0 mmol), and TsOH (0.1 mmol), was added dioxane (7 mL) at room temperature. The mixture was heated under reflux for 9 h, then concentrated under reduced pressure, and the residue was purified by column chromatography on silica gel using ethyl acetate (16%–20%)/petroleum ether as eluent to afford the final product.

2,2'-[(9,9-Dimethyl-9*H*-fluorene-2,7-diyl)bis(4,1-phenylene)]bis(1*H*-benz[*d*]imidazole) (14a) This compound was obtained from **7** and **10a**; yellow solid; yield 65%; mp > 400°C; $^1\text{H-NMR}$ ($\text{DMSO}-d_6$): δ 8.31 (d, $J = 9.5$ Hz, 4H), 8.04 (m, 8H), 7.82 (dd, $J_1 = 1.4$ Hz,

$J_2 = 2.6$ Hz, 2H), 7.69 (br, 2H), 7.56 (br, 2H), 7.23 (br, 2H), 1.63 (s, 6H); $^{13}\text{C-NMR}$ ($\text{DMSO}-d_6$): δ 155.1, 151.4, 142.0, 139.0, 138.4, 129.4, 127.6, 127.4, 126.4, 121.6, 121.3, 79.7, 79.4, 79.1, 47.3, 27.3; λ_{abs} (CH_2Cl_2) 360 nm, λ_{abs} (MeOH) 348 nm; λ_{em} (CH_2Cl_2) 457 nm, λ_{em} (MeOH) 401 nm and 426 nm, λ_{em} (film) 462 nm. HR-MS. Calcd for $\text{C}_{41}\text{H}_{30}\text{N}_4$ ($[\text{M}+\text{H}]^+$): m/z 579.2548. Found: m/z 579.2530.

2,2'-[(9,9-Dimethyl-9*H*-fluorene-2,7-diyl)bis(4,1-phenylene)]bis(1-phenyl-1*H*-benz[*d*]imidazole) (14b) This compound was obtained from **7** and **10b**; white solid; yield 75%; mp 318–32°C; $^1\text{H-NMR}$ (CDCl_3): δ 7.94 (d, $J = 8.3$ Hz, 2H), 7.80 (d, $J = 8.4$ Hz, 2H), 7.51–7.72 (m, 19H), 7.39 (m, 6H), 7.30 (m, 3H), 1.58 (s, 6H); $^{13}\text{C-NMR}$ (CDCl_3): δ 154.6, 152.0, 142.8, 142.3, 139.3, 138.4, 137.3, 137.0, 130.0, 129.9, 129.8, 128.6, 128.5, 127.5, 126.9, 126.2, 123.4, 123.1, 121.2, 120.5, 119.7, 110.4, 47.1, 27.3; λ_{abs} (CH_2Cl_2) 360 nm, λ_{abs} (MeOH) 340 nm; λ_{em} (CH_2Cl_2) 493 nm, λ_{em} (MeOH) 402 nm and 425 nm, λ_{em} (film) 450 nm. HR-MS. Calcd for $\text{C}_{53}\text{H}_{38}\text{N}_4$ ($[\text{M}+\text{H}]^+$): m/z 731.3174. Found: m/z 731.3169.

2,2'-[(9,9-Dimethyl-9*H*-fluorene-2,7-diyl)bis(4,1-phenylene)]bis(1-(4-methoxyphenyl)-1*H*-benz[*d*]imidazole) (14c) This compound was obtained from **7** and **10c**; white solid; yield 70%; mp 294–296°C; $^1\text{H-NMR}$ (CDCl_3): δ 7.92 (d, $J = 7.2$ Hz, 2H), 7.81 (d, $J = 8.3$ Hz, 2H), 7.73 (d, $J = 8.5$ Hz, 4H), 7.64 (m, 8H), 7.23–7.39 (m, 10H), 7.07 (d, $J = 9.4$ Hz, 4H), 3.92 (s, 6H), 1.59 (s, 6H); $^{13}\text{C-NMR}$ (CDCl_3): δ 159.6, 154.6, 152.1, 142.2, 139.3, 138.4, 137.7, 129.8, 129.6, 128.6, 126.9, 126.2, 123.3, 123.0,

Table 2 Crystal data and structure refinement for **11b** and **13b**.

	11b	13b
Empirical formula	$\text{C}_{44}\text{H}_{46}\text{N}_2$	$\text{C}_{42}\text{H}_{44}\text{N}_2\text{S}$
Formula weight	602.83	608.85
Temperature	296(2) K	296(2) K
Wavelength	0.71073 Å	0.71073 Å
Crystal system, space group	Triclinic, $P\bar{1}$	Triclinic, $P\bar{1}$
a (Å)	8.8196(12)	8.849(2)
b (Å)	11.3574(14)	11.872(3)
c (Å)	18.332(2)	17.588(4)
α (°)	79.002(3)	101.232(7)
β (°)	85.340(3)	90.384(7)
γ (°)	85.257(4)	102.640(6)
Volume (Å ³)	1792.3(4)	1766.0(7)
Z	2	2
Density (calc.) (mg/m ³)	1.117	1.145
Absorption coefficient (mm ⁻¹)	0.064	0.122
$F(000)$	648	652
Crystal size (mm)	0.175 × 0.158 × 0.079	0.211 × 0.089 × 0.076
θ range for data collection (°)	1.831–25.049	1.795–25.495
Limiting indices	$-10 \leq h \leq 10$, $-11 \leq k \leq 13$, $-21 \leq l \leq 21$	$-10 \leq h \leq 10$, $-14 \leq k \leq 10$, $-18 \leq l \leq 21$
Reflections collected/unique	10157/6296 [$R(\text{int}) = 0.0397$]	10410/6549 [$R(\text{int}) = 0.0395$]
Completeness to $\theta = 25.05$	97.5%	99.8%
Absorption correction	Semi-empirical from equivalents	Semi-empirical from equivalents
Max. and min. transmission	0.7457 and 0.6580	0.7457 and 0.6015
Refinement method	Full-matrix least-squares on F^2	Full-matrix least-squares on F^2
Data/restraints/parameters	6331/89/483	6549/98/465
Goodness-of-fit on F^2	1.038	0.996
Final R indices [$I > 2\sigma(I)$]	$R_1 = 0.0853$, $wR_2 = 0.2188$	$R_1 = 0.0691$, $wR_2 = 0.1699$
R indices (all data)	$R_1 = 0.1569$, $wR_2 = 0.2548$	$R_1 = 0.1290$, $wR_2 = 0.2030$
Absolute structure parameter	0.004(2)	0.008(4)
Largest diff. peak and hole (eÅ ⁻³)	0.275 and -0.243	0.380 and -0.219

121.2, 120.5, 119.7, 115.1, 110.4, 55.5, 29.7, 27.3; λ_{abs} (CH₂Cl₂) 350 nm, λ_{em} (MeOH) 346 nm; λ_{em} (CH₂Cl₂) 463 nm, λ_{em} (MeOH) 402, 425 nm, λ_{em} (film) 452 nm. HR-MS. Calcd for C₅₅H₄₂N₄O₂ ([M + H]⁺): m/z 791.3386. Found: m/z 791.3346.

2,2'-[(9,9-Dimethyl-9H-fluorene-2,7-diyl)bis(furan-5,2-diyl)]bis(1H-benz[d]imidazole) (15a) This compound was obtained from **8** and **10a**; yellow-brown solid; yield 68%; mp > 400°C; ¹H-NMR (CDCl₃): δ 8.16 (s, 2H), 8.00 (q, J = 27.7 Hz, 4H), 7.63 (br, 4H), 7.37 (d, J = 3.3 Hz, 2H), 7.30 (d, J = 3.3 Hz), 7.23 (q, J = 9.3 Hz, 4H), 1.63 (s, 6H); ¹³C-NMR (CDCl₃): δ 155.1, 154.9, 145.3, 144.0, 138.5, 129.3, 121.4, 118.8, 113.3, 108.8, 47.2, 27.3; λ_{abs} (CH₂Cl₂) 394 nm, λ_{abs} (MeOH) 390 nm; λ_{em} (CH₂Cl₂) 463 nm, λ_{em} (MeOH) 403 nm and 425 nm, λ_{em} (film) 427 nm. HR-MS. Calcd for C₅₇H₂₆N₄O₂ ([M + H]⁺): m/z 559.2134. Found: m/z 559.2119.

2,2'-[(9,9-Dimethyl-9H-fluorene-2,7-diyl)bis(furan-5,2-diyl)]bis(1-phenyl-1H-benz[d]imidazole) (15b) This compound was obtained from **8** and **10b**; brown solid; yield 67%; mp 242–250°C; ¹H-NMR (DMSO-*d*₆): δ 7.90 (d, J = 9.3 Hz, 2H), 7.72 (m, 6H), 7.64 (d, J = 8.5 Hz, 2H), 7.55 (m, 4H), 7.26–7.43 (m, 8H), 7.15 (d, J = 8.4 Hz, 2H), 6.93 (d, J = 4.2 Hz, 2H), 6.76 (d, J = 3.1 Hz, 2H), 1.51 (s, 6H); ¹³C-NMR (DMSO-*d*₆): δ 155.9, 154.4, 144.1, 142.9, 138.5, 137.0, 129.8, 129.3, 128.8, 128.1, 123.5, 123.5, 123.2, 120.2, 119.5, 118.0, 115.2, 110.2, 107.0, 47.1, 29.7; λ_{abs} (CH₂Cl₂) 420 nm, λ_{abs} (MeOH) 394 nm; λ_{em} (CH₂Cl₂) 470 nm and 500 nm, λ_{em} (MeOH) 402 nm and 427 nm, λ_{em} (film) 437 nm. HR-MS. Calcd for C₄₉H₄₄N₄O₂ ([M + H]⁺): m/z 711.2760. Found: m/z 711.2755.

2,2'-[(9,9-Dimethyl-9H-fluorene-2,7-diyl)bis(thiophene-5,2-diyl)]bis(1H-benz[d]imidazole) (16a) This compound was obtained from **9** and **10a**; yellow solid; yield 62%; mp > 400°C; ¹H-NMR (DMSO-*d*₆): δ 7.99 (d, J = 1.5 Hz, 2H), 7.96 (d, J = 8.8 Hz, 2H), 7.87 (d, J = 4.3 Hz, 2H), 7.76 (dd, J_1 = 1.5 Hz, J_2 = 2.4 Hz, 2H), 7.74 (d, J = 4.3 Hz, 2H), 7.59 (br, 4H), 7.22 (s, 4H), 1.59 (s, 6H); ¹³C-NMR (DMSO-*d*₆): δ 155.1, 147.2, 146.3, 138.5, 133.0, 128.2, 125.2, 121.3, 120.4, 47.3, 29.4, 27.2; λ_{abs} (CH₂Cl₂): 400 nm, λ_{abs} (MeOH): 393 nm; λ_{em} (CH₂Cl₂): 496 nm, λ_{em} (MeOH): 436 nm. HR-MS. Calcd for C₃₇H₂₆N₄S₂ ([M + H]⁺): m/z 591.1667. Found: m/z 591.1669.

2,2'-[(9,9-Dimethyl-9H-fluorene-2,7-diyl)bis(thiophene-5,2-diyl)]bis(1-phenyl-1H-benz[d]imidazole) (16b) This compound was obtained from **9** and **10b**; yellow solid; yield 60%; mp 112–116°C; ¹H-NMR (CDCl₃): δ 7.91 (s, 2H), 7.43–7.72 (m, 16H), 7.05–7.41 (m, 9H), 6.88 (s, 1H), 1.53 (s, 6H); ¹³C-NMR (CDCl₃): δ 154.6, 147.9, 146.9, 138.7, 137.5, 136.1, 132.7, 130.6, 130.3, 130.1, 129.8, 129.6, 128.3, 128.2, 125.1, 123.9, 123.5, 123.4, 120.6, 120.2, 119.1, 114.0, 110.1, 47.0, 29.7, 27.1; λ_{abs} (CH₂Cl₂): 418 nm, λ_{abs} (MeOH): 393 nm; λ_{em} (CH₂Cl₂): 482 nm, λ_{em} (MeOH): 445, 472 nm. HR-MS. Calcd for C₄₉H₄₄N₄S₂ ([M + H]⁺): m/z 743.2303. Found: m/z 743.2293.

X-ray structural analysis of 11b and 13b

Suitable single crystals of **11b** and **13b** for X-ray structural analysis were obtained by slow concentration of solution in chloroform at room temperature. The selected crystals with approximate dimensions of 0.19 × 0.15 × 0.03 mm for **11b** and 0.211 × 0.089 × 0.076 mm for **13b** were mounted on a four-circle single crystal X-ray diffractometer (CAD4 DIFFRACTIS 586). A graphite monochromated MoK α radiation (λ = 0.071073 nm) was used and the data were collected

at 296 (2) K. The structure was solved by direct methods and refined by full-matrix least-squares method on F_{obs}^2 using the SHELXTL 97 software package. The non-hydrogen atoms were refined anisotropically. The hydrogen atoms bound to carbon were located by using geometrical calculations, with their position and thermal parameters being fixed during the structure refinement. A summary of the crystallographic data and structure refinement details are given in Table 2.

Acknowledgments: The authors are grateful for supports from the National Natural Science Foundation of China (Project No. 81202402 and 21272154). The authors also thank Drs. H. Deng and M. Shao, The Instrumental Analysis & Research Center of Shanghai University, for structural analysis.

References

- [1] Tao, S.; Li, L.; Yu, J.; Jiang, Y.; Zhou, Y.; Lee, C. S. Bipolar molecule as an excellent hole-transporter for organic-light emitting devices. *Chem. Mater.* **2009**, *21*, 1284–1287.
- [2] Rouxel, C.; Charlot, M.; Mir, Y.; Frochot, C.; Mongin, O.; Blancharddesce, M. Banana-shaped biphotonic quadrupolar chromophores: from fluorophores to biphotonic photosensitizers. *New J. Chem.* **2011**, *35*, 1771–1780.
- [3] Moura, G. L. C.; Simas, A. M. Two-photon absorption by fluorene derivatives: systematic molecular design. *J. Phys. Chem. C* **2010**, *114*, 6106–6116.
- [4] Andrade, C. D.; Yanez, C. O.; Rodriguez, L.; Belfield, K. D. A series of fluorene-based two-photon absorbing molecules: synthesis, linear and nonlinear characterization, and bioimaging. *J. Org. Chem.* **2010**, *75*, 3975–3982.
- [5] Wang, H. L.; Li, Z.; Shao, P.; Qin, J. G.; Huang, Z. L. Two-photon absorption property of a conjugated polymer: influence of solvent and concentration on its property. *J. Phys. Chem. B* **2010**, *114*, 22–27.
- [6] Grimsdale, A. C.; Chan, K. L.; Martin, R. E.; Jokisz, P. G.; Holmes, A. B. Synthesis of light-emitting conjugated polymers for applications in electroluminescent devices. *Chem. Rev.* **2009**, *109*, 897–1091.
- [7] Muroga, T.; Sakaguchi, T.; Hashimoto, T. Synthesis and photoluminescence properties of heterocycle-containing poly(disubstituted acetylene)s. *Polymer* **2012**, *53*, 4380–4387.
- [8] Cao, X. Y.; Zhang, W.; Pei, J. π -Conjugated twin molecules based on truxene: synthesis and optical properties. *Org. Lett.* **2004**, *6*, 4845–4848.
- [9] Zhao, Z. J.; Xu, X. J.; Jiang, Z. T.; Lu, P.; Yu, G.; Liu, Y. Q. Oligo(2,7-fluorene ethynylene) with pyrene moieties: synthesis, characterization, photoluminescence, and electroluminescence. *J. Org. Chem.* **2007**, *72*, 8345–8353.
- [10] Liao, Y. L.; Lin, C. Y.; Wong, K. T.; Hou, T. H.; Hun, Y. W. A novel ambipolar spirobifluorene derivative that behaves as an efficient blue-light emitter in organic light-emitting diodes. *Org. Lett.* **2007**, *9*, 4511–4514.
- [11] Lee, J. F.; Chen, Y. C.; Lin, J. T.; Wu, C. C.; Chen, C. Y.; Dai, C. A.; Chao, C. Y.; Chen, H. L.; Liao, W. B. Blue light-emitting and electron-transporting materials based on dialkyl-functionized

- anthracene imidazophenanthrolines. *Tetrahedron* **2011**, *67*, 1696–1702.
- [12] Zhang, Y.; Lai, S. L.; Tong, Q. X.; Chan, M. Y.; Ng, T. W.; Wen, Z. C.; Zhang, G. Q.; Lee, S. T.; Kwong, H. L.; Lee, C. S. Synthesis and characterization of phenanthroimidazole derivatives for applications in organic electroluminescent devices. *J. Mater. Chem.* **2011**, *21*, 8206–8214.
- [13] Wang, C. L.; Dong, H. L.; Hu, W. P.; Liu, Y. Q.; Zhu, D. B. Semi-conducting pi-conjugated systems in field-effect transistors: a material odyssey of organic electronics. *Chem. Rev.* **2012**, *112*, 2208–2267.
- [14] He, G. S.; Tan, L. S.; Zheng, Q. D.; Prasad, P. Multiphoton absorbing materials: molecular designs, characterizations, and applications. *Chem. Rev.* **2008**, *108*, 1245–1330.
- [15] Hung, L. S.; Chen, C. H. Recent progress of molecular organic electroluminescent materials and devices. *Mater. Sci. Eng. R.* **2012**, *39*, 143–222.
- [16] Snaith, H. J.; Greenham, N. C.; Friend, R. H. The origin of collected charge and open-circuit voltage in blended polyfluorene photovoltaic devices. *Adv. Mater.* **2004**, *16*, 1640–1645.
- [17] Werts, M. H. W.; Gmouh, S.; Mongin, O.; Pons, T.; Desce, M. Strong modulation of two-photon excited fluorescence of quadripolar dyes by (de)protonation. *J. Am. Chem. Soc.* **2004**, *126*, 16294–16295.
- [18] Zhou, X. H.; Yan, J. C. Exploiting an imidazole-functionalized polyfluorene derivative as a chemosensory material. *J. Macromolecules* **2004**, *37*, 7078–7080.
- [19] Zhang, Y.; Lai, S. L.; Tong, Q. X.; Lo, M. F.; Ng, T. W.; Chan, M. Y.; Wen, Z. C.; He, J.; Jeff, K. S.; Tang, X. L. High efficiency nondoped deep-blue organic light emitting devices based on imidazole- π -triphenylamine derivatives. *Chem. Mater.* **2012**, *24*, 61–70.
- [20] Li, W. J.; Liu, D. D.; Shen, F. Z.; Ma, D. G.; Wang, Z. M.; Feng, T.; Xu, Y. X.; Yang, B.; Ma, Y. G. A twisting donor-acceptor molecule with an intercrossed excited state for highly efficient, deep-blue electroluminescence. *Adv. Funct. Mater.* **2012**, *22*, 2797–2803.
- [21] Kulkarni, A. P.; Tonzola, C. J.; Babel, A.; Jenekhe, S. A. Electron transport materials for organic light-emitting diodes. *Chem. Mater.* **2004**, *16*, 4556–4573.
- [22] Kuo, C. J.; Li, T. Y.; Lien, C. C.; Liu, C. H.; Wu, F. I.; Huang, M. J. Bis(phenanthroimidazolyl)biphenyl derivatives as saturated blue emitters for electroluminescent devices. *J. Mater. Chem.* **2009**, *19*, 1865–1871.
- [23] Wang, Z. M.; Lu, P.; Chen, S. M.; Gao, Z.; Shen, F. Z.; Zhang, W. S.; Xu, Y. X.; Kwok, H. S.; Ma, Y. G. Phenanthro[9,10-*d*]imidazole as a new building block for blue light emitting materials. *J. Mater. Chem.* **2011**, *21*, 5451–5456.
- [24] Lai, M. Y.; Chen, C. H.; Huang, W. S.; Lin, J. T.; Ke, T. H.; Chen, L. Y.; Tsai, M. H.; Wu, C. Benzimidazole/amine-based compounds capable of ambipolar transport for application in single-layer blue-emitting OLEDs and as hosts for phosphorescent emitters. *Angew. Chem. Int. Ed.* **2008**, *47*, 591–595.
- [25] Jenekhe, S. A.; Osaheni, J. A. Excimers and exciplexes of conjugated polymers. *Science* **1994**, *265*, 765–768.
- [26] Han, J.; An, J.; Im, C.; Cho, N. S.; Shim, H. K.; Majima, T. Comparing electroluminescence efficiency and photoluminescence quantum yield of fluorene based pi-conjugated copolymers with narrow band-gap comonomers. *J. Photochem. Photobiol. A.* **2009**, *205*, 98–103.
- [27] Setayesh, S.; Grimsdale, A. C.; Weil, T.; Enkelmann, V.; Müllen, K.; Meghdadi, F.; List, E. J. W.; Leising, G. Polyfluorenes with polyphenylene dendron side chains: toward non-aggregating, light-emitting polymers. *J. Am. Chem. Soc.* **2001**, *123*, 853–946.
- [28] Marsitzky, D.; Scott, J. C.; Chen, J. P.; Lee, V. Y.; Miller, R. D.; Setayesh, S.; Mullen, K. Poly-2,8-(indeno[fluorene-co-anthracene) colorfast blue-light-emitting random copolymer. *Adv. Mater.* **2001**, *13*, 1096–1100.
- [29] Li, Z. H.; Wong, M. S.; Fukutani, H.; Tao, Y. Full emission color tuning in bisdipolar diphenyl amino-encapped oligoaryl fluorenes. *Chem. Mater.* **2005**, *17*, 5032–5040.
- [30] Yasuda, T.; Fujita, K.; Tsutsui, T. Carrier transport properties of monodisperse glassy-nematic oligofluorenes in organic field-effect transistors. *Chem. Mater.* **2005**, *17*, 264–268.
- [31] Lai, W. Y.; Zhu, R.; Fan, Q. L.; Hou, L. T.; Cao, Y.; Huang, W. Monodisperse sixarmed triazatruxenes: microwave-enhanced synthesis and highly efficient pure-deep-blue electroluminescence. *Macromolecules* **2006**, *39*, 3707–3970.
- [32] Chen, H. F.; Cui, Y. M.; Guo, J. G.; Lin, H. X.; Synthesis and optical properties of 6,10-dihydrofluoreno[2,3-*d*:6',7'-*d'*]diimidazole derivatives. *Dyes Pigm.* **2012**, *94*, 583–591.
- [33] Guo, J. G.; Cui, Y. M.; Lin, H. X.; Xie, X. Z.; Chen, H. F. New fluorene derivatives based on 3,9-dihydrofluoreno[3,2-*d*]imidazole (FI): Characterization and influence of substituents on photoluminescence. *J. Photochem. Photobiol. A: Chem.* **2011**, *219*, 42–49.
- [34] Hao, Z. S.; Li, M. J.; Lin, H. X.; Gu, Z. B.; Cui, Y. M. Synthesis, optical and electrochemical properties of 2,3-diphenyl-10H-indeno[1,2-*g*]quinoxaline, 15H-dibenzo[*a,c*]indeno[1,2-*i*]phenazine and 15H-indeno[1,2-*i*]phenanthro[4,5-*abc*]phenazine derivatives. *Dyes Pigm.* **2014**, *109*, 54–66.
- [35] Gu, Z. B.; Lin, H. X.; Cui, Y. M.; Li, M. J.; Hao, Z. S. Synthesis and characterization of 2',7'-diarylspiro[cyclopentane-1,9'-fluorene] derivatives. *Monatsh. Chem.* **2015**, *146*, 1519–1527.
- [36] Jiang, Y.; Wang, J. Y.; Ma, Y.; Cui, Y. X.; Zhou, Q. F.; Pei, J. Large rigid blue-emitting π -conjugated stilbenoid-based dendrimers: synthesis and properties. *Org. Lett.* **2006**, *8*, 4287–4290.
- [37] Kumar, D.; Thomas, K. R. J.; Lin, C. C.; Jou, J. H. Pyrenoimidazole-based deep-blue-emitting materials: optical, electrochemical, and electroluminescent characteristics. *Chem. Asian J.* **2013**, *8*, 2111–2124.
- [38] Mulhern, K.; Detty, M.; Watson, D. Aggregation-induced increase of the quantum yield of electron injection from chalcogenorhodamine dyes to TiO₂. *J. Phys. Chem. C.* **2011**, *115*, 6010–6018.
- [39] Adachi, K.; Mita, T.; Yamate, T.; Yamazaki, S.; Takechi, H.; Watarai, H. Controllable adsorption and ideal H-aggregation behaviors of phenothiazine dyes on the tungsten oxide nanocolloid surface. *Langmuir* **2010**, *26*, 117–125.
- [40] Chen, S.; Raad, F. S.; Ahmida, M.; Kaafarani, B. R.; Eichhorn, S. H. Columnar mesomorphism of fluorescent board-shaped quinoxalino-phenanthrophenazine derivatives with donor-acceptor structure. *Org. Lett.* **2013**, *15*, 558–561.
- [41] Feng, X.; Iwanaga, F.; Hu, J. Y.; Tomiyasu, H.; Nakano, M.; Redshaw, C.; Elsegood, M. R. J.; Yamato, T. An efficient approach to the synthesis of novel pyrene-fused azaacenes. *Org. Lett.* **2013**, *15*, 3594–3597.
- [42] Thomas, J.; Tyag, P. Synthesis, spectra, and theoretical investigations of the triarylamines based on 6H-indolo[2,3-*b*]quinoxaline. *J. Org. Chem.* **2010**, *75*, 8100–8111.